Facile Chemical Modification of Aquivion® Membranes for Anionic Fuel Cells

Simone Bonizzoni,[a] Pietro Stilli,[a] Felix Lohmann-Richters,[b] Claudio Oldani,[c] Chiara Ferrara,[a] Antonio Papagni,[a] Luca Beverina,[a] and Piercarlo Mustarelli*[a]

Anion-exchange membranes (AEMs) are of growing interest for electrochemical devices such as fuel cells and electrolyzers because the alkaline medium allows avoiding the use of platinum and platinum-group metals as the electrocatalysts. Perfluorinated polymers are a good starting point to prepare AEMs because of their chemical stability and potential high conductivity resulting from the coexistence of hydrophobic main chains and flexible hydrophilic side chains. Here, we report a facile and simple chemical modification of Aquivion® performed in aqueous environment. We obtained a chemically stable membrane with ionic conductivity exceeding 2.5×10^{-2} S cm^{-1} at 80 °C and 100 RH% that was used in a polymer fuel cell.

Introduction

Hydrogen is an essential driver to lead our overall society towards climate neutrality by boosting decarbonization in the power and transport sectors as well as in the energy intensive industry. Concerning the EU, hydrogen is expected to supply up to 20% of energy demand by 2050.[1] The ongoing radical refurbishing of the EU energy infrastructure and transportation aims to promote the widespread adoption of renewable energy sources.[2,3] Most are at such stage of development that it is impossible to predict which, if any, will be prevalent.[4,5] Thus, it is essential to pursue a range of approaches including several sectors: electricity generation and storage, transportation, and industrial use. One of the most promising ways to achieve these objectives is involving innovative electrochemical energy conversion and storage systems, *e.g.* fuel cells (FCs) and water electrolyzers (WEs).[5] These devices are very attractive for their high conversion efficiency and negligible emissions of greenhouse gases. However, FCs and WEs can achieve high current densities only with high-performance membrane-electrode assemblies (MEAs).[6]

To date, proton exchange membrane fuel cells (PEMFCs) and proton exchange membrane water electrolyzers (PEMWEs) employ membranes based on perfluorinated ionomers (PFI) with a very high conductivity, chemical and electrochemical stability.[7–9] Nevertheless, PFIs suffer from relevant drawbacks: i) high cost, ii) higher crossover with respect to other systems, e.g. polybenzimidazoles, both in case of H_2[10] and methanol as the fuel,[11] and iii) the need of Pt-group metals (PGMs) as the electrocatalysts, which is chiefly due to the acidic environment.[12]

To address such issues, anion-exchange membranes (AEMs) have been proposed.[13] AEMs give rise to a highly alkaline environment at the electrodes, and the mechanisms of the electrochemical reactions are very different in comparison with those occurring in the acidic medium.[14] Consequently, the rate-determining electrochemical processes can be efficiently promoted also by PGM-free ECs.[15] AEMs are typically based on polyelectrolytes built with polymers such as poly(arylene ethers), polybenzimidazoles, unsaturated polypropylene and polyethylene, polystyrene and poly(vinylbenzyl chloride).[16] The charged groups consist mostly of quaternary ammoniums, imidazoliums, benzimidazoliums, pyridiniums, phosphonium, sulfonium cations, and metal-based systems that can include more than one positive charge per side chain.[13,16,17] However, state-of-the-art AEMs still suffer from significant shortcomings. The main issues are indeed their limited chemical stability in OH- form, and their ionic conductivity, which is low for practical applications as the mobility of OH^- ions is lower than that of H^+ in conventional PFI membranes.[13,18] Thus, AEMs with a very high ion-exchange capacity (IEC) are needed. Nevertheless, a high IEC typically results in poor mechanical properties and excessive swelling upon hydration.[19] Another drawback of AEMs in the OH^- form is carbonation upon exposure to CO_2 traces, which compromises their conductivity and, in turn, reduces the devices performance.[13] Finally, the durability of AEMs is still insufficient.[19–21] Some of these drawbacks can be overcome by a proper tailoring of the membrane, e.g. i) by developing phase-segregated AEMs comprising hydrophobic

[a] S. Bonizzoni, P. Stilli, Dr. C. Ferrara, Prof. A. Papagni, Prof. L. Beverina, Prof. P. Mustarelli
University of Milano Bicocca
Via Cozzi 55, 20125, Milano, Italy
E-mail: piercarlo.mustarelli@unimib.it
[b] Dr. F. Lohmann-Richters
Forschungszentrum Jülich GmbH
Institute of Energy and Climate Research
IEK-14: Electrochemical Process Engineering
52428 Jülich, Germany
[c] Dr. C. Oldani
Solvay Specialty Polymers (Italy) S.p.A.
Viale Lombardia 20, 20021 Bollate, Milano (Italy)

Supporting information for this article is available on the WWW under https://doi.org/10.1002/celc.202100382

phases enhancing mechanical properties, inter-dispersed into hydrophilic phases which promote ion conduction,[22] ii) cross-sslinked AEMs, which reduce crossover,[23] and iii) hybrid inorganic-organic AEMs, comprising a nanofiller dispersed in a polymeric matrix.[24]

Recently, several groups reported on the preparation of perfluorinated polymers containing quaternary ammonium groups from Nafion®- and Aquivion®-based sulfonyl fluoride precursors to give anion exchange membranes.[25–28] In this paper, for the first time to the best of our knowledge, we report on the chemical modification of the sulphonated form of Aquivion® to obtain a chemically stable AEM for application in anion-conducting fuel cells and electrolyzers. We performed a thorough physico-chemical characterization of the membrane and demonstrated the preliminary fabrication of MEAs with good functional properties.

Experimental Section

Raw Materials

Aquivion® membranes (E98-12S, EW = 980 g eq^{-1}, 120 μm) and dispersion (**D72**-25BS) were obtained by Solvay Specialty Polymers S.p.a. (Italy). N,N,2,2-tetramethyl-1,3-propanediamine (hereinafter diamine), iodomethene, potassium hydroxide, sodium chloride, silver nitrate, sodium nitrate, potassium chromate, methanol, ethanol, *N*-Methyl-2-pyrrolidone and acetonitrile were obtained by Merck. Carbon paper (Sigracet 22 BB), alkaline membrane (Fumapem FAA-3-50), alkaline ionomer (Fumapem FAA-3 solution 10% NMP), Pt black and Pt-Ru black 1:1 as anodic and cathodic catalysts, respectively, were obtained by Fuel Cell Store (USA).

Polymer Functionalization

The AEM was obtained starting from Aquivion® with the following steps: sulfonamide bond formation (Steps 1a and 1b), methylation (Step 2) and ionic exchange (Step 3).

The Step 1a (see Scheme 1) consists in the acid-base reaction between sulfonic group and primary amine giving their salt. In a typical reaction, 400 mg of membrane were soaked in water for one hour, then a 5-fold excess of amine was added and let to react for 1 day at room temperature. The sample was recovered, washed with ethanol and dried under vacuum at 50 °C for one hour.

The Step 1b is the conversion of the salt in the corresponding sulfonamide by thermally induced dehydration (Scheme 2). The membranes were treated at 250 °C for 1 hour according with the TGA results (see following).

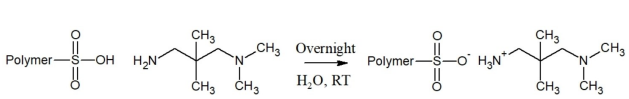

Scheme 1. Step 1a

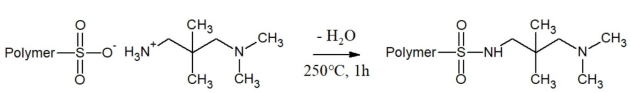

Scheme 2. Step 1b

In Step 2, the diamine was converted in the corresponding tetraalkylammonium salt by reaction with excess methyl iodide (10:1 excess). The membranes were soaked in anhydrous acetonitrile for one hour and then an excess of iodomethane was added and let to react for 14 hours at 40 °C in a pressure tight vessel. After that, the sample was recovered, washed with acetonitrile and water and dried under vacuum at 80 °C for 1 hour (Scheme 3).

Finally, in Step 3 the iodide-form membrane was immersed in 1 M KOH water/ethanol 1:1 solution for one day in order to exchange anions. The sample was then washed with water and dried in vacuum at 80 °C for 1 hour under vacuum (Scheme 4).

The anion membrane was stored in a home-made wet box (65% RH) under controlled nitrogen atmosphere (CO_2 less than 5 ppm). Pictures of the membrane after the various steps are reported in Supplementary Information (Figure S1).

Membrane Characterization

The ion-exchange capacity (IEC) of the membrane was determined by the Mohr titration method.[29] A strip 2×4 cm^2 of AEM was immersed in a 0.5 M NaCl solution for 24 h, washed in water for 5 h and then immersed in a 0.2 M $NaNO_3$ solution for 24 h. Finally, the $NaNO_3$ solution was titrated with a 0.01 M $AgNO_3$ standard solution using K_2CrO_4 as the indicator. The membrane was dried at 120 °C under vacuum for 2 h and weighed. The IEC was calculated as the ratio of the milliequivalents of membrane and its dry mass as following formula:

$$IEC\left(\frac{meq}{g}\right) = \frac{Stoichiometric\ volume\ (mL)^{*}Conc.\ AgNO_3\ \left(\frac{meq}{mL}\right)}{dry\ mass\ (g)}$$

The in-plane conductivity of AEMs was determined by means of Electrochemical Impedance Spectroscopy using a VSP-300 multi-channel (Biologic), with a 4-electrodes conductivity cell mounted in Fuel Cell Test System 850e (Scribner). The home-made, four-electrodes cell is made with Teflon®. The electrodes are made of Pt wire 0.6 mm in diameter. The distance between the inner contacts is 0.5, the distance between the outer contacts is 1.8 cm. An image of the cell is reported in Figure S2. Before the measurements, the membrane was activated by immersion in KOH 1 M for one night, and then washed three times in pure water. The measurements were carried out under nitrogen flux at 80 °C in the frequency range 100 Hz–1 MHz, and in the relative humidity range 60%–100%.

Solid state NMR data were collected for each step reported in the schemes of the reaction on an Avance III Bruker 400 MHz spectrometer (9.4 T magnet) using a 4 mm MAS probe. ^1H spectra were collected with a single-pulse sequence adopting a π/2 pulse of 2.5 ms, the delay time was checked for each sample and

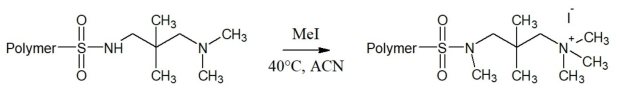

Scheme 3. Step 2

Scheme 4. Step 3

averaged over 128 scans under MAS conditions (10 kHz). ^{13}C spectra were acquired with ^{13}C-^{1}H CP-MAS sequence under the same MAS conditions. The ^{1}H $\pi/2$ pulse was 2.5 ms, the delay time 5–200 s depending on the sample, as previously determined with ^{1}H experiments, the contact time 2.5 ms, and the signals were averaged over 1k–8k acquisitions. Chemical shifts for both ^{1}H and ^{13}C have been referred to adamantane signals as a secondary standard with respect to tetramethylsilane (TMS, 0 ppm). The spectra were acquired, processed and analyzed with the software package Topspin 3.1 (Bruker).

The Infrared (IR) spectra were obtained on Jasco FT/IR-4100 spectrometer equipped with ATR accessory and the data were analyzed with Spectra Manager™ Suite software. The measurements were recorder from 4000–500 cm^{-1} with resolution of 2.0 cm^{-1}.

Simultaneous DSC/TGA experiments were performed by means of a TGA/DSC 1 star® system (Mettler Toledo). The TGA measurements were carried out by heating the samples up to 600 °C, with a heating rate of 10 °C/min in N_2 flux. DSC measurements were performed under N_2 flux with the following procedure: from 25 °C to 280 °C at 10 °C/min, 3 min at 280 °C, from 280 °C to 25 °C, 3 min at 25 °C and from 25 °C to 280 °C.

The chemical stability of the final membrane was checked by evaluating the ionic conductivity at 80 °C and 100% RH after immersion, for different times, in 6 M KOH aqueous solution under stirring at 25 °C in wet-box.

SEM images were acquired with a Gemini 500 Microscope (Zeiss). Samples were coated with graphite before of the experiments.

Electrodes and MEA Fabrication

The electrodes (2.1 × 2.1 cm^2) were prepared by casting drop-by-drop on carbon paper (Sigracet B22) an ink made by Pt black and PtRu black (equimolar) as the ECs, and a Fumapem FAA-3 solution 10%NMP dispersion as the ionomer. The amounts of ECs were defined to obtain a Pt surface density of 0.2 mg cm^{-2} on both the electrodes. A 10 wt% excess was considered to allow for losses during the deposition process. The ionomer was activated, as suggested by the producer, by soaking it in 1 M KOH solution for 3 days. The electrocatalyst, ionomer and isopropanol were mixed for 4 minutes by ultrasonication (Fisher Scientific).

The MEA was assembled by pressing the membrane and the electrodes at the room temperature, directly inside the cell fixture (Scribner). A torque of 4.5 Nm was applied to the cell screws. The polarization curves were recorded using a Fuel Cell Test System 850e (Scribner) equipped with a 885-HS potentiostat (Scribner). Measurements were carried out by potentiodynamic experiments, sweeping from OCV to 0.3 V at 80 °C, 100% RH, with hydrogen and air, both 100% humidified, with volume ratio 1:5 H_2:air. No back-pressure was applied. The hydrogen was produced by a SHC Hydrogen Generator.

Results and Discussion

The procedure of Aquivion® functionalization was investigated by solid-state NMR and IR spectroscopies. Figure 1 reports the ^{1}H-^{13}C CP-MAS spectra of the samples after the steps reported in the Experimental Section. The peak (a) is due to the backbone fluorinated carbons of Aquivion®. The low intensity of this signal is due to the absence of ^{1}H-^{13}C cross-polarization.

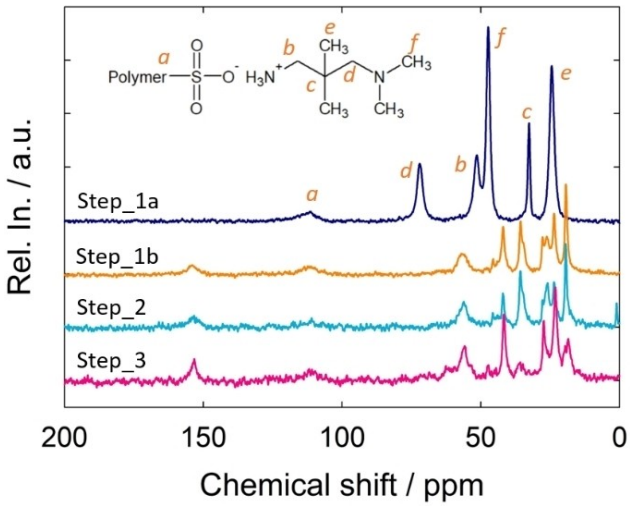

Figure 1. ^{13}C-^{1}H CP-MAS NMR spectra of the different steps of the functionalization reaction. The peaks assignment after the Step 1a is reported in the Figure. Step 1a: salification, Step 1b: salt dehydration, Step 2: methylation, Step 3: OH exchange.

The attribution of the diamine NMR peaks is performed in agreement with the high-resolution spectrum in solution reported by the AIST database.[30] The small peak in the range 150–160 ppm for the samples Step 1b, Step 2 and Step 3 is due to carbonyl groups originated by reactions with CO_2 residuals in the atmosphere-controlled oven used for the thermal treatment in Step 1b.

The formation of the covalent –S–N– bond after Step 1b is clearly demonstrated by the upfield shift of all the peaks (b–e) attributed to the diamine. The small contributions in the range 25–30 ppm are likely due to non-equivalent sites in the crystal structure. The further steps, included the formation of additional methyl groups linked to the two nitrogen atoms, induce only minor changes in the NMR spectrum, but for some variation of the intensities of the involved peaks. The complete assignment of the NMR peaks in steps 1b–3 is difficult. In fact, whereas it was simple to state the chemical reaction between the sulphonic unit and the amine took place (because of the overall upfield shift of the amine peaks), the exact correlation of the peaks b–f of Figure 1 with the diamine carbon is not straightforward because of attraction effects, and would require a detailed computational (e.g. Density Functional Theory, DFT) study, which is outside the aim of this study. The different intensities of the signal due to the backbone carbons (peak a) are due to unequal efficiency of the ^{1}H-^{13}C cross-polarization, which may be influenced by several physico-chemical properties, including sample crystallinity, polymer viscosity, etc.

The success of the functionalization reaction is confirmed by the IR analysis. Figure 2 shows the IR spectra for the pristine Aquivion®, the diamine and the membrane after Step 3. The pristine material shows the characteristic signals of the fluorinated backbone, such as the $–CF_2–$ stretching at 1320, 1200 and 1146 cm^{-1}, and the $–SO_3$ side chain stretching at 1278 and 1056 cm^{-1}, and the C–O–C stretching at 966 cm^{-1}.[31] The water adsorbed gives two typical signals at 3500 and 1630 cm^{-1}

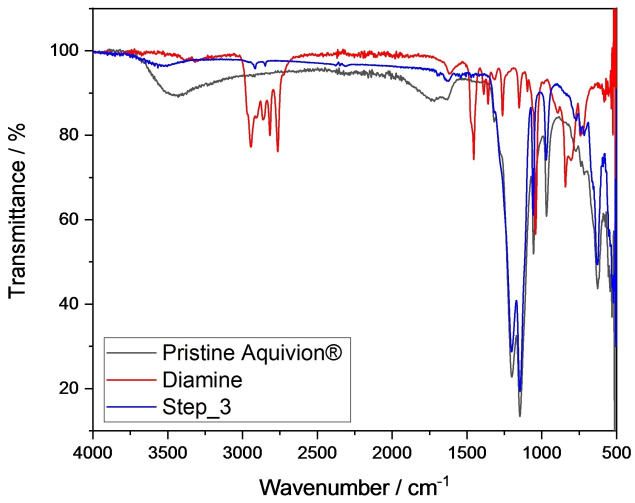

Figure 2. FTIR spectra of the pristine Aquivion® (black), the N,N,2,2-tetramethyl-1,3-propandiamine (red), and the membrane after Step 3 (blue). The curves are shifted for the sake of clearness.

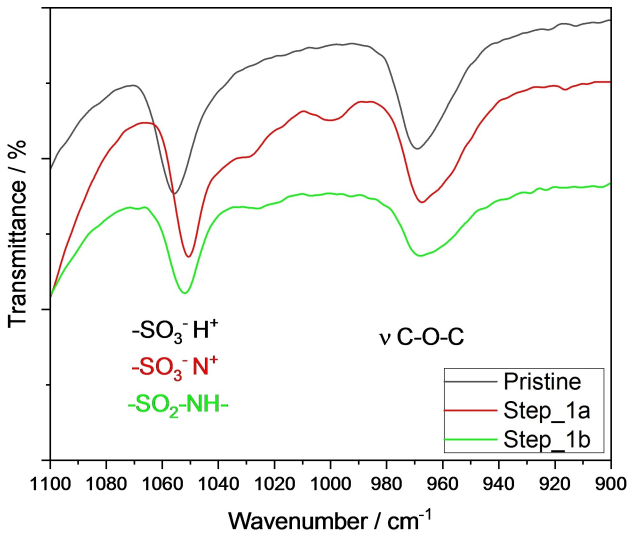

Figure 3. IR spectra of samples after Step 1a and Step 1b in the region 1100–900 cm^{-1}.

due to the stretching and bending of O–H bond, while the H_3O^+ bending gives a signal at 1720 cm^{-1}.[32] Here we note that the C–F transitions are very strong and, therefore, they might cover other signals in the 1400–1000 cm^{-1} zone. For this reason, in order to follow the structure changes, we have monitored the $-SO_3$ stretching at 1056 cm^{-1}, which can shift depending by the different cations.[33] The diamine spectrum shows the N–H stretching at 3390 and 3316 cm^{-1},[34] the C–H stretching of the $-CH_3$ at 2970 and 2860 cm^{-1}, of the $-CH_2-$ at 2944 and 2816 cm^{-1}, and of the N–CH_3 group at 2764 cm^{-1}.[35,36] The signals given by the C–H bending of the CH_3 and CH_2 are visible at 1475, 1455, 1388, 1360, 1315 cm^{-1} as reported in Ref. [34]. In the fingerprint zone there are also the C–N stretching at 1141 cm^{-1}[36] and the N–H wagging at 840 cm^{-1}.[35] In the spectrum of the membrane after Step 3 there are the main signals of Aquivion® polymer, such as CF_2 and SO_3 groups transition in 1400–900 zone, as well as the stretching and bending of C–H of CH_3 groups correlated to amine fragment at 1475 and 1455 cm^{-1}. There is a signal at 1698 cm^{-1} that we correlated to the partial carbonation process which is also visible in NMR spectra above 150 ppm (see Figure 1). Full IR peaks assignment is reported in Table S1.

As stated, in order to obtain a clearer insight of the functionalization process we investigated in more detail the $-SO_3$ stretching at ~1050–1060 cm^{-1}. Figure 3 shows the spectra of samples after Step 1a and Step 1b in the region 1100–900 cm^{-1}. The $-SO_3$ stretching signal shifts from 1056 to 1051 and to 1052 cm^{-1} for Step 1a and Step 1b, respectively. The first shift is correlated to the exchange of proton by charged diamine, while the second one proves the sulfonamide bond formation according to Lee et al.[25]

Figure 4a shows the TGA curves of the pristine membrane and the products obtained after the Steps 1a, 1b, 2 and 3. The pristine membrane showed a loss of ~5 wt% below 170 °C due to moisture release, and then a multi-step thermal degradation starting at ~300 °C. During the reaction steps, the thermal stability progressively increased to ~350 °C thanks to sulfonamide bond, and finally reached ~450 °C for the final OH^--form membrane.

The most interesting thermal behavior was observed for the sample after Step 1 a (red curve, see also the inset). With reference to the inset, we observed an initial weight loss of 0.5 wt% in the range 25–100 °C which is due to absorbed moisture (region I). After this, there is a flat region up to 130 °C (II), followed by a weight loss of 2 wt% in the region 130–245 °C (III), which is likely due water release caused by sulfonamide bond formation. Indeed, the loss of 2 wt% corresponds to nearly complete reaction, given the equivalent and molecular weights of Aquivion® (1108 g/mol) and diamine (130.26 g/mol), respectively. The loss of water in this step was confirmed by TG/FTIR measurements (see Supplementary Information, Figure S3). Finally, there was a loss of 1 wt% in the range 245–260 °C which is attributed to the degradation of unreacted diamine (region IV). This is also confirmed by TG/FTIR measurements reported in Figure S3. A 1 wt% decrease corresponds to a reaction yield of 88.2%, in excellent agreement with the IEC results, which gave an overall functionalization yield of 91.4% (see Experimental Section).

Figure 4b shows the DSC curves of the sample after Step 1a subjected to two subsequent heating cycles. During the first cycle, non-reversible endotherms corresponding to the TGA losses of regions I, III and IV can be clearly observed. These endotherms are not present in the second cycle.

The IEC value obtained for the membrane after Step 3 was 0.77 meq g^{-1}, to be compared with the value of the Aquivion® membrane in its proton-conducting form (0.86 meq g^{-1}). We also tested the IEC after ageing the membrane 69 days in KOH 6 M solution at r.t., and obtained a value of 0.63 meq g^{-1}.

Figure 5 shows the behavior of the ionic conductivity at 80 °C vs. the relative humidity for the Aquivion® membrane in its H^+ form, and for the anion-conducting ones after the Steps 2 and 3, which means in iodide and hydroxide form,

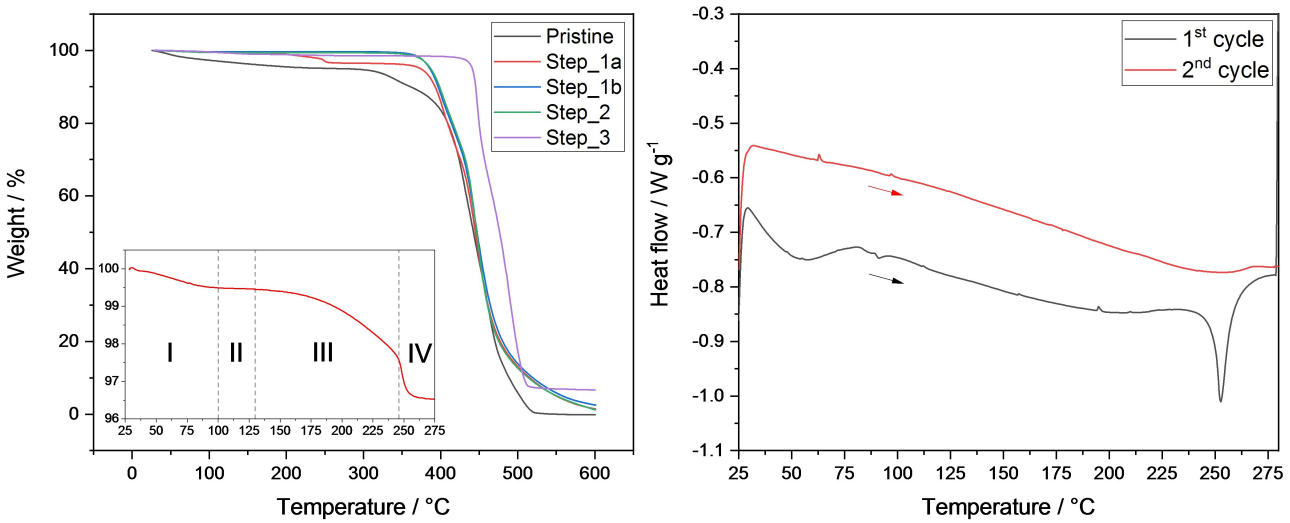

Figure 4. a) TGA curves of the samples after all the reaction steps. The inset shows the weight loss below 275 °C of the sample after the Step 1a; b) DSC curves of the sample after the Step 1a.

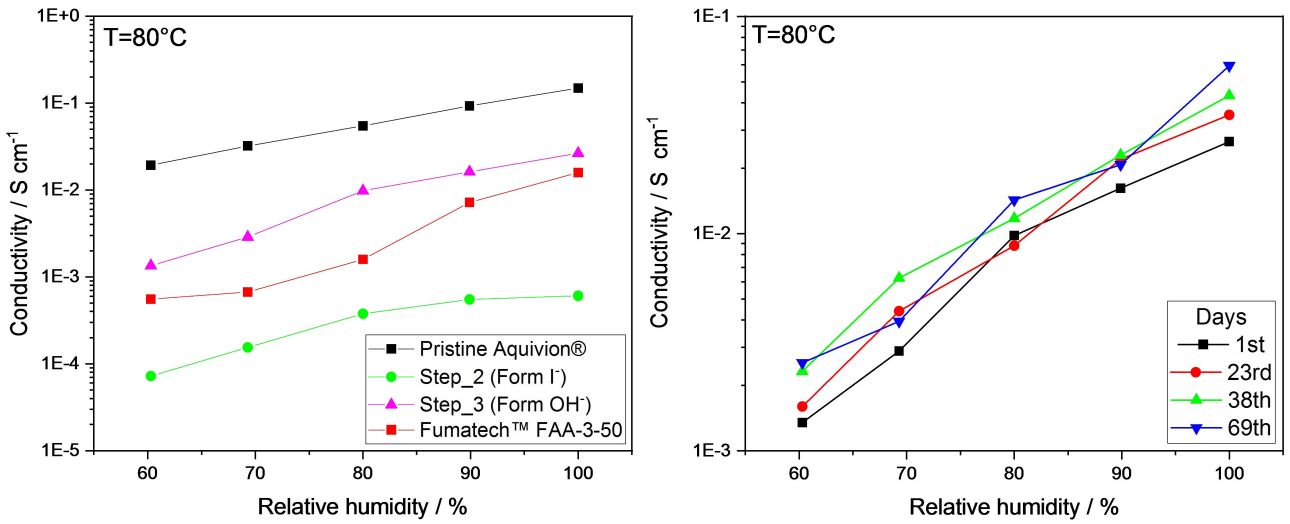

Figure 5. a) Ionic conductivity of pristine Aquivion® in its H^+ form, iodide-form and hydroxide-form membranes vs. the relative humidity at 80 °C. The conductivity of the Fumapem FAA-3-50 reference membrane is reported for the sake of comparison. b) Behaviour vs. time of the ionic conductivity of the hydroxide-form membrane kept in KOH 6 M aqueous solution at room temperature for 23, 38 and 69 days, and then measured at 80 °C.

respectively. The conductivity of Fumapem FAA-3-50 membrane is shown for the sake of comparison. As expected, the anion-conducting membranes showed values lower than the protonic one because of the lower mobility of I^- and OH^- with respect to H^+. However, the hydroxide form (Step 3) showed an ionic conductivity of 2.6×10^{-2} S cm^{-1} at 100 RH%, which is better than that of the commercial Fumapem FAA-3-50 reference membrane tested under the same conditions.[25] Figure 5b shows some preliminary results about the stability of the ionic conductivity of the hydroxide-form membrane upon long-term immersion in 6 M KOH solution at the room temperature.

The as-produced membrane presents an ionic conductivity of 2.6×10^{-2} S cm^{-1} at 80 °C and 100% relative humidity. After 69 days of storage in KOH 6 M aqueous solution at room temperature, this value increases by more than a factor of two to 5.9×10^{-2} S cm^{-1}. We note that the conductivity at 100% relative humidity increases monotonously with the ageing time. Whereas we have not a clear-cut explanation for this, a possible cause could be a modification of the membrane microstructure. Figure S4 shows the cross-sectional SEM images of the membrane as-prepared, and of the same sample kept 69 days in 6 M KOH solution at the room temperature. As a matter of fact, the comparison shows that the aged membrane has a more open structure, which may somehow reduce its tortuosity. This, indeed, could also cause an increase of the membrane gas permeability, which will be addressed in further studies.

The task to determine the chemical stability of anionic membranes deserves great attention.[13] In fact, simple determination of conductivity after ageing is not enough, and this information must be complemented with a range of additional

measurements, including IEC after harsh ageing at temperatures in the range 80–90 C, and spectroscopic investigations (NMR, IR, Raman) both before and after ageing. Figure S5 shows the comparison of Electrochemical Impedance Spectroscopy (EIS) between the as-prepared membrane (after Step 3) and the same membrane kept 6 days at 80 C in KOH 6 M solution. We observe that the two samples display roughly the same bulk resistance. The ionic conductivity of the membrane after the ageing treatment is 2.9×10^{-2} S cm^{-1} at 80 °C and 100 % RH, to be compared with 2.6×10^{-2} S cm^{-1} of Figure 5a. Finally, Figure S6 shows the comparison of the IR spectra of the membrane as prepared and after kept 6 days at 80 C in KOH 6 M solution. The two spectra appear very similar. Consequently, we can conclude that the membrane has good stability in alkaline environment, at least in the limits of the ageing protocol we employed.

Finally, Figure 6 shows the polarization curve of a MEA prepared as described in the Experimental Section. A maximum power density of the order of 50 mW cm^{-2} was obtained. However, these data should be intended as preliminary, as no optimization was yet performed on electrode preparation and MEA assembly. Among the possible optimization strategies, we highlight: i) the use in the ink of an ionomer made by the same modified Aquivion® employed in the membrane; ii) a better dispersion of the ionomer in the ink, iii) the use of carbon cloth instead of carbon paper and, iv) the use of hot-pressing for MEA assembly, in order to improve the mechanical contact among the compartments. A subsequent publication will report on the performance under electrolyzing conditions.

Conclusions

In this paper we reported a facile and sustainable method to obtain anion-conducting membranes starting from the sulphonated moiety of Aquivion®, one of the market references in the sector of proton-conducting membranes. The choice of sulphonated Aquivion® allowed us to avoid all the issues related to hydrofluoric acid formation in starting from the $-SO_2F$ form. The final hydroxide-form membrane showed good ionic conductivity and high chemical stability. Preliminary fuel cell tests gave a maximum power density of 50 mW cm^{-2} under conditions which still need to be optimized.

We stress that a correct evaluation of the advantages of our Aquivion®-based membrane with respect to, e.g., less expensive hydrocarbons-based ones will require check long-term stability and performance under operating conditions. This work is in progress and will be the subject of a future publication.

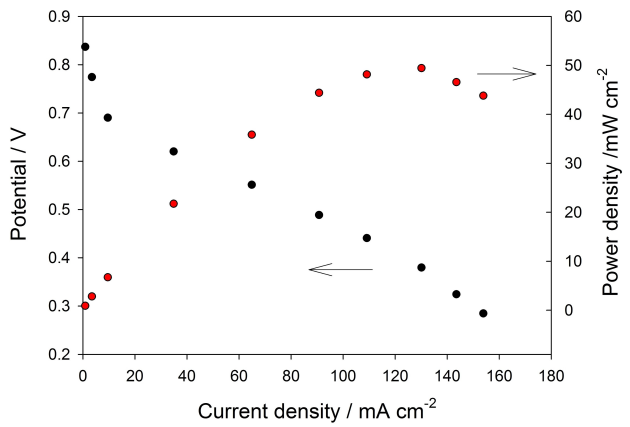

Figure 6. Polarization curve of the MEA with the AEM. Measurements were carried out by potentiodynamic experiments, sweeping from OCV to 0.3 V at 80 °C, 100 % RH, with hydrogen and air, both 100 % humidified, with volume ratio 1 : 5 H_2 : air. No back-pressure was applied at the electrodes.

Acknowledgements

Financial support from the Ministry of University and Research (MIUR) through FISR "AMPERE" project (cod. FISR2019_01294) is gratefully acknowledged. We also thank MIUR for the grant Dipartimenti di Eccellenza – 2017 "Materials For Energy". The work of S.B. is performed in the frame of his PhD. The work of P.S. is performed in the frame of his Master Degree.

Conflict of Interest

The authors declare no conflict of interest.

Keywords: anion-exchange membranes · fuel cells · electrolyzers · ionic conductivity · stability

[1] https://emiri.eu/uploads/content files/65/value file/EMIRI%20Technology%20Roadmap%20-%20September%202019%20(cond).pdf.
[2] Energy 2020, COM(2010) 639, Brussels, 2010.
[3] Energy infrastructure priorities for 2020 and beyond, COM(2010) 677, Brussels, 2010.
[4] Investing in the Development of Low Carbon Technologies (SET-Plan), SEC(2009) 1295, Brussels, 2009.
[5] Technology Map of the European SET-Plan Brussels, 2011.
[6] M. Breitwieser, M. Klingele, S. Vierrath, R. Zengerle, S. Thiele, *Adv. Energy Mater.* **2018**, *8*, 1701257.
[7] V. Di Noto, T. A. Zawodzinski, A. M. Herring, G. A. Giffin, E. Negro, S. Lavina, *Int. J. Hydrogen Energy* **2012**, *37*, 6120–6131.
[8] A. Z. Weber, M. M. Mench, J. P. Meyers, P. N. Ross, J. T. Gostick, Q. Liu, *J. Appl. Electrochem.* **2011**, *41*, 1137–1164.
[9] C. Spiegel, Designing and Building Fuel Cells, 1st ed., McGraw-Hill, New York, 2007.
[10] Q. Li, J. O. Jensen, R. F. Savinell, N. J. Bjerrum, *Prog. Polym. Sci.* **2009**, *34*, 449–477.
[11] A. Carollo, E. Quartarone, C. Tomasi, P. Mustarelli, F. Belotti, A. Magistris, F. Maestroni, M. Parachini, L. Garlaschelli, P. P. Righetti, *J. Power Sources* **2006**, *160*, 175–180.
[12] J. Zhang, *Front. Energy Res.* **2011**, *5*, 137–148.
[13] J. R. Varcoe, P. Atanassov, D. R. Dekel, A. M. Herring, M. A. Hickner, P. A. Kohl, A. R. Kucernak, W. E. Mustain, K. Nijmeijer, K. Scott, T. Xuk, L. Zhuang, *Energy Environ. Sci.* **2014**, *7*, 3135–3191.
[14] N. Ramaswamy, S. Mukerjee, *J. Phys. Chem. C* **2011**, *115*, 18015–18026.
[15] S. Gottesfeld, D. R. Dekel, M. Page, C. Bae, Y. Yan, P. Zelenay, Y. S. Kim, *J. Power Sources* **2018**, *375*, 170–184.
[16] K. Vezzù, A. M. Maes, F. Bertasi, A. R. Motz, T.-H. Tsai, E. B. Coughlin, A. M. Herring, V. Di Noto, *J. Am. Chem. Soc.* **2018**, *140*, 1372–1384.
[17] D. Henkensmeier, M. Najibah, C. Harms, J. Zitka, J. Hnat, K. Bouzek, *J. Electrochem. Energy Conv. Stor.* **2021**, *18*, 024001–1.
[18] D. Marx, A. Chandra, M. E. Tuckerman, *Chem. Rev.* **2010**, *110*, 2174–2216.
[19] Y. J. Wang, J. Qiao, R. Baker, J. Zhang, *Chem. Soc. Rev.* **2013**, *42*, 5768–5787.

[20] H. Long, K. Kim, B. S. Pivovar, *J. Phys. Chem. C* **2012**, *116*, 9419–9426.
[21] J. B. Edson, C. S. Macomber, B. S. Pivovar, J. M. Boncella, *J. Membr. Sci.* **2012**, *399–400*, 49–59.
[22] N. Li, M. D. Guiver, *Macromolecules* **2014**, *47*, 2175–2198.
[23] S. D. Poynton, J. P. Kizewski, R. C. T. Sladel, J. R. Varcoe, *Solid State Ionics* **2010**, *181*, 219–222.
[24] M. T. Pérez-Prior, T. García-García, A. Várez, B. Levenfeld, *J. Mater. Sci.* **2015**, *50*, 5893–5903.
[25] S. Lee, H. Lee, T.-H. Yang, B. Bae, N. A. T. Tran, Y. Cho, N. Jung, D. Shin, *Membranes* **2020**, *10*, 306–318.
[26] S. Petricci, P. A. Guarda, C. Oldani, G. Marchionni, Patent WO2012/098146.
[27] C. Oldani, L. Merlo, Patent WO2012/136688.
[28] M. A. Vandiver, J. L. Horan, Y. Yang, E. T. Tansey, S. Seifert, M. W. Liberatore, A. M. Herring, *J. Polym. Sci. Part B* **2013**, *51*, 1761–1769.
[29] E. Kim, S. Lee, S. Woo, S.-H. Park, S.-D. Yim, D. Shin, B. Bae, *J. Power Sources* **2017**, *359*, 568–576.
[30] https://sdbs.db.aist.go.jp/sdbs/cgi-bin/cre index.cgi.
[31] M. Danilczuk, L. Lin, S. Schlick, S. J. Hamrock, M. S. Schaberg, *J. Power Sources* **2011**, *196*, 8216–8224.
[32] M. Laporta, M. Pegoraro, L. Zanderighi, *Phys. Chem. Chem. Phys.* **1999**, *1*, 4619–4628.
[33] S. R. Lowry, K. A. Mauritz, *J. Am. Chem. Soc.* **1980**, *102*, 4665–4667.
[34] P. J. Krueger, *Can. J. Chem.* **1967**, *45*, 2143–2149.
[35] N. Ozturk, S. Bahceli, *Z. Naturforsch.* **2006**, *61a*, 399–401.
[36] J. Hine, W.-S. Li, *J. Org. Chem.* **1975**, *40*, 289–292.

Manuscript received: March 23, 2021
Revised manuscript received: May 31, 2021
Accepted manuscript online: May 31, 2021